

Performance of One-Dimensional Multilayer Nanostructure Emitter and Filter for Thermophotovoltaic applications

Samah G. Babiker^{1*}, Mohamed O. Sid-Ahmed², Shuai Yong³
and Xie Ming³

¹*Department of Physics -Faculty of Education, University of the Holy Quran and Islamic Science-Omdurman-Sudan*

²*Department of Physics -Faculty of Science, Sudan University of Science and Technology, Khartoum- Sudan*

³*Department of Engineering Thermophysics-School of Energy Science and Engineering, Harbin Institute of Technology, Box. 456, 92 West DaZhi Street, NanGang District, Harbin City, P.R. China Zip Code: 150001*

samahgas@yahoo.com

Abstract

In this paper, a one - dimensional multilayer is optimized for potential applications as thermophotovoltaic (TPV) selective emitter and filter. Both of the proposed structures were prepared through a magnetron sputtering process. The influence of multilayer selective emitter and filter on the radiative properties is studied by using the rigorous coupled-wave analysis (RCWA). The emittance spectrum of the proposed TPV selective emitter shows three emittance peaks which are explained by the surface plasmon polariton (SPP), gap Plasmon polariton (GPP) and magnetic polariton (MP) excitation. The results show that the proposed emitter has high net radiation power. The calculated results show that the proposed filter has high transmittance for photons at $\lambda \leq 1.73\mu\text{m}$. The TPV system with a selective emitter and filter and GaSb photovoltaic cell has a potential to be used as a power a generator.

Keywords: *Thermophotovoltaic, Selective emitter, Filter, Rigorous Coupled-Wave Analysis (RCWA)*

1. Introduction

The depleting fossil fuel reserves require looking for solutions such as new sources of energy, high energy conversion efficiency and recycling of waste heat by using of alternative energy sources. Thermophotovoltaic (TPV) systems provide a viable solution for fulfilling these requirements [1-2]. Thermophotovoltaic (TPV) systems are capable of converting thermal infrared radiation into electricity without involving any moving parts, by using photovoltaic effect. The concept of TPV dates back to 1960s. It was only in recent years that technological improvements in the field of low band gap (0.50 - 0.75 eV) photovoltaic cells, such as GaSb, GaInAs and GaInAsSb cells, and high temperature selective emitting materials, have evoked a renewed interest in TPV generation of electricity [1, 3-4]. The TPV system basically consists of a thermal radiator (emitter), a filter and a low band gap photovoltaic PV cell. The TPV system promises to be a very clean and quiet source of electrical power, with good reliability, portable, with no moving parts (so low maintenance), high output power density. It can be used as stand-alone system for power production in combustion equipment.

As a result, TPV system can be more commonly used in many applications such as recycling waste energy from industrial processes, electric-grid independent appliances, military applications, cogeneration of heat and electricity in domestic boilers [5-7]. However, the most obvious drawbacks of TPV systems are their low throughput and poor conversion efficiency, due to a large amount of unusable radiation [1, 8]. A TPV system receives radiation either as broad - or narrow- band from a heat source at a much lower temperature than the sun surface temperature and at a distance of only a few centimeters. A highly efficient TPV system demands the optimization of the output power and throughput. The emitter temperature in a TPV system generally ranges between 1000 and 2000 K. This implies that the largest part of radiation is emitted in the infrared range of the electromagnetic spectrum, instead of the visible range according to (Wien's displacement law). The optimum bandgap for source temperature is given by Shockley and Queisser's hallmark [9]. Photons having energies higher than the TPV cell bandgap would be absorbed within the depletion region and could produce electricity. Photons having energies less than the TPV cell bandgap (sub-band gap photons) would be absorbed beyond the depletion region and cannot produce electricity. These sub-bandgap photons will result in a destructive heat load on the system components, which will lower the conversion efficiency of the system. In order to reduce the heating and to improve the TPV overall efficiency, these photons should be sent back to the emitter by using filters and back surface reflectors [1, 10]. Recently near-field thermal radiation has been proposed to enhance the throughput and the conversion efficiency by bringing the emitter and TPV cell in close proximity [11], while the conversion efficiency can be improved by controlling the emission spectrum and directions. One possible solution to increase their conversion efficiency and output power is to apply microscale radiation principles in TPV systems. The output power can be increased by using micro/nanostructures in the TPV components emitter and filter. This reduces the amount of unusable radiation [12]. The throughput can also be increased by using micro/nanostructures, because it reduces the distance between the emitter and the TPV cell to sub-wavelength dimensions [13].

Periodic micro/nanostructures in one, two or three dimensional (1D, 2D, or 3D) can enhance the conversion efficiency through the modification of the radiative properties of the electromagnetic waves and thermal emission spectrum [14-15]. Several researchers have used micro/nanostructures as emitter and filter to enhance TPV efficiency, based on different physical mechanisms such as one-dimensional 1D deep gratings which enhance the emission via excitation of surface plasmon polaritons (SPPs) [16], 1D photonic crystal (PhC) [17] and 2D microcavities which enhance the emission via cavity resonance (CR) modes [18]. A 3D tungsten photonic crystal [12] and 3D metallic woodpile have recently been used as thermophotovoltaic emitter [19]. Multilayer microstructures have also been proposed to control thermal radiation [20].

1D photonic crystals consisting of dielectric - dielectric multilayer (Si/SiO₂) and 1D metallic - dielectric (Ag/SiO₂) were used as filters in both thermophotovoltaic and micro thermophotovoltaic systems [21, 22]. In this paper, we propose 1D 4-layer (W/SiO₂) and 1D 8-layer (Si/SiO₂) as selective emitter and filter, respectively to improvement TPV system performance. The influence of a selective emitter and filter on the spectral radiative properties was studied by using numerical calculations rigorous coupled wave analysis (RCWA) method [23].

2. Calculation Method

Rigorous coupled-wave analysis (RCWA) is formulated in the 1980s by Moharam and Gaylord. It is used for analyzing the diffraction of electromagnetic waves by periodic gratings [24]. RCWA is used in this study to calculate the radiative properties

(emittance and transmittance) of the periodically multilayer surfaces. It analyzes the general diffraction problem by solving Maxwell's equations accurately in each of the three regions (input, multilayer, and output), based on Fourier expansion [23]. In RCWA, diffraction efficiency for each diffraction order is calculated with incident wave properties regardless of feature size, structural profiles, and dielectric function of the materials. The dielectric function of the materials is expressed as $\varepsilon = (n + ik)^2$, where n is the refractive index and k is the extinction coefficient. The accuracy of the solution computed depends solely upon the number of terms retained in space harmonic expansion of electromagnetic fields, which corresponds to the diffraction order. The emittance is calculated from the reflectance according to Kirchhoff's law. Any linearly-polarized incidence can be decomposed into the transverse electric (TE) and transverse magnetic (TM) mode. The normalized electric field of incidence E_{inc} can be expressed as:

$$E_{inc} = \exp(ik_x x + ik_z z - i\omega t) \quad (1)$$

The electric field in region I (Figure. 1a) is the superposition of the incident wave and the reflected waves; therefore

$$E_I(x, z) = \exp(ik_x x + ik_z z) + \sum_j E_{ij} \exp(ik_{xj} x - ik_{zj}^r z) \quad (2)$$

Similarly, the electric field in region IV (E_{IV}) is the a superposition of all transmitted waves

$$E_{IV}(x, z) = \sum_j E_{ij} \exp(ik_{xj} x - ik_{zj}^t z) \quad (3)$$

The magnetic field H in region I and IV can be obtained from Maxwell's equation

$$H_I(x, z) = -\frac{i}{\omega\mu_0} (\nabla \times E_I) \quad (4)$$

$$H_{IV}(x, z) = -\frac{i}{\omega\mu_0} (\nabla \times E_{IV}) \quad (5)$$

where ω represents the frequency and μ_0 the magnetic permeability of vacuum. The electric and magnetic field components in region M (Figure.1a) can be expressed as a Fourier series:

$$E_M(x, z) = \sum_j \chi_{yj}(z) \exp(ik_{xj} x) y \quad (6)$$

$$H_M(x, z) = \frac{ik}{\omega\mu_0} \sum_j [\gamma_{xj}(z)x + \gamma_{zj}(z)z] \exp(ik_{xj} x) \quad (7)$$

where χ_{yj} and γ_{xj} are vector components for the j th space-harmonic electric and magnetic field in region M (multilayer region), respectively. ϵ_0 is the electric permittivity in vacuum. Due to the structure periodicity, the relative dielectric function in region M, $\epsilon(x)$ and its inverse, $1/\epsilon(x)$ can also be expanded in Fourier series:

$$\epsilon(x) = \sum_p \epsilon_p^{ord} \exp\left(i \frac{2p\pi}{\Lambda} x\right) \quad (8)$$

$$\frac{1}{\epsilon(x)} = \sum_p \epsilon_p^{inv} \exp\left(i \frac{2p\pi}{\Lambda} x\right) \quad (9)$$

where ϵ_p^{ord} and ϵ_p^{inv} are the j th Fourier coefficient for the ordinary and inverse of $\epsilon(x)$, respectively.

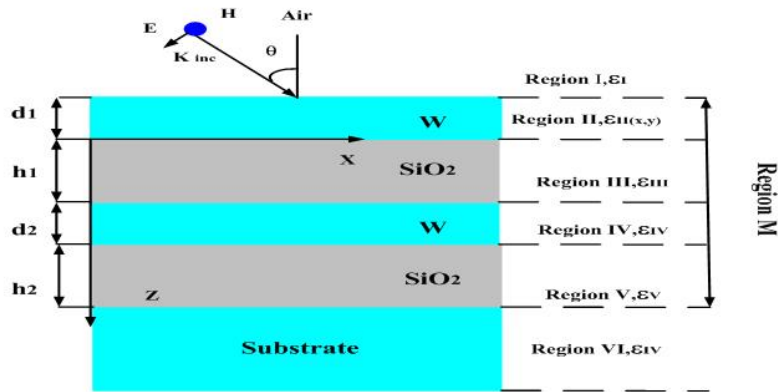
3. The Proposed Thermophotovoltaic System

3.1. Selective emitter

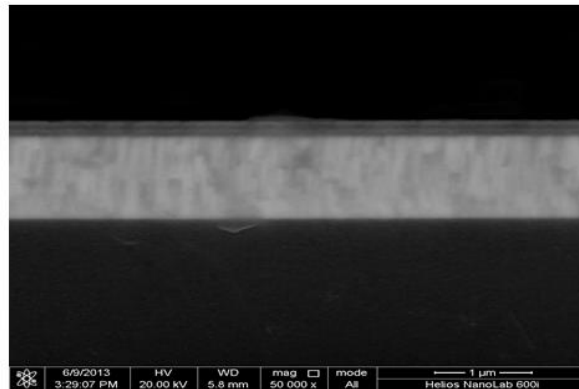
The emitter is one of the main components in the TPV system. There are basically two different types of emitters, namely broadband emitters such as blackbody (BB) and silicon carbide (SiC), or selective emitters. The selective emitter is characterized by strong emission at certain wavelengths and low elsewhere. It can be made from wavelength selective emitting materials either by tailoring the material properties of the emitter through doping and alloying such as $\text{Er}_3\text{Al}_5\text{O}_{12}$ (erbia) or by the use of microstructured surfaces [1, 10]. A TPV system uses an emitter, which is heated up by various energy sources to high temperatures, as a source of radiation for photovoltaic energy conversion, but in most cases it is heated by chemical energy [2, 25]. That means a large amount of unusable electromagnetic radiation impinges on the photovoltaic cell (PV) [2]. So, the enhancement of TPV efficiency can be achieved by using selective emitters [26]. An ideal TPV emitter should have high emissivity close to unity corresponding to the spectral region, where a TPV cell has high quantum efficiency and as low as possible outside that region. It also needs to be polarization-insensitive so that high emissivity for both transverse electric wave (TE wave or s-polarization) and transverse magnetic wave (TM wave or p-polarization) can be achieved. Tungsten is usually used as a suitable metal in the emitter fabrication due to its high melting point, good corrosion resistance and its ability to withstand high temperatures [1-2, 16]. Tungsten emitters have relatively low emissivity in the mid- and far-infrared region due to free electrons. 1D periodic gratings TPV emitter was proposed by Chen and Zhang [16] (complex grating as a wavelength selective emitter) and by Narayanaswamy and Chen [17] (photonic crystal (PhC) made of tungsten and alumina as a wavelength selective emitter). Development of 2D structure includes tungsten gratings emitter with thermally excited surface plasmons polaritons (SPPs) [27]. A 3D tungsten photonic crystal [28] and 3D metallic woodpile as a TPV emitter were recently fabricated with an efficiency which exceeds 32% [19].

In this paper we investigate the spectral emittance of a 1D periodic multilayer selective emitter. The proposed selective emitter consists of four layers atop a substrate and the image of the scanning electron microscope (SEM) is shown in Figure 1. The layers are made of tungsten (W) and silicon dioxide (SiO_2). The geometric parameters used to illustrate the

wavelength selective TPV emitter are the thickness of the layers $d_1 = h_1 = 60\text{nm}$, $d_2 = 20\text{nm}$, $h_2 = 400\text{nm}$ and the entire structure is deposited on an opaque tungsten film. The wavelength-dependent dielectric optical constants of tungsten and silicon dioxide were obtained from Ref [29].



(a)



(b)

Figure 1. (a)Schematic of the proposed a TPV emitter made of multilayer tungsten and silicon dioxide; (b) The image of the SEM

3.2. Selective filter

The proposed TPV selective filter is a 1D- eight-layer system in the form of (Si/SiO_2) was also prepared through a magnetron sputtering process and the image of the SEM of the system are shown in Figure 2. The thickness of the Si layer is 160 nm and that of the SiO_2 layer is 440 nm. They were deposited on a quartz substrate. The refractive index of Si and SiO_2 are taken to be 3.4 and 1.5, respectively.

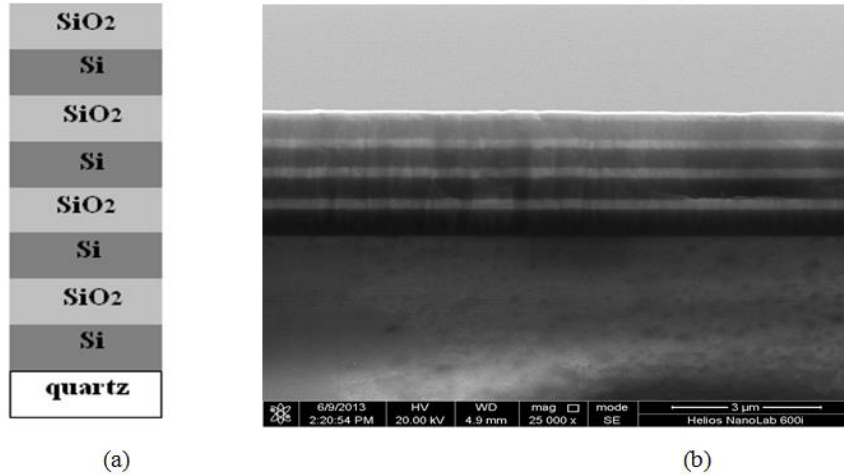


Figure 2. (a) The proposed TPV selective filter; (b) SEM image

4. Results and Discussion

4.1. Spectral emittance and BRDF measurements for the proposed TPV emitter

The spectral emittance of the TPV selective emitter and of the plain tungsten, at near normal incidence 8^0 for TE and TM waves, is shown in Figure 3. The spectral emittance for the proposed TPV selective emitter was measured experimentally by using spectral transmittance and reflectance measurement system in the wavelength range from $0.3 \mu\text{m}$ to $2.5 \mu\text{m}$ and exhibits high value about 0.62 and 0.94 for TE and TM waves, respectively. It also calculated numerically by using RCWA method in the wavelength range from $0.5 \mu\text{m}$ to $5 \mu\text{m}$ and shows high value in the spectral range of $0.69 < \lambda < 1.97 \mu\text{m}$ and its decreases below 0.2 at $\lambda \geq 3.06 \mu\text{m}$ for TM wave. Three peaks (> 0.9) on the emittance occur in the spectral range of $0.69 < \lambda < 1.97 \mu\text{m}$. The first peak at $0.81 \mu\text{m}$ occurs due to excitation of the surface plasmon polaritons (SPPs) at the air-tungsten interface, which is confirmed by its polariton dispersion curves those depends on the relative permittivity or dielectric function (i.e. optical constants). The second peak at $\lambda = 1.13 \mu\text{m}$ occurs due to the interband absorption in tungsten. The (W/SiO₂/W) waveguide can support the propagation of the gap plasmon polaritons (GPPs) mode. The third peak at $\lambda = 1.76 \mu\text{m}$ is attributed to the excitation of magnetic polaritons (MPs). The excitation of the MPs mode can strongly localize the electromagnetic energy into the dielectric layer which is inserted between the top tungsten layer and tungsten substrate. Although, the emissivity values at these peaks experimentally higher than simulation results, this is attributed to the influence of the sample by experiment environment or due to the samples fabrication errors at preparation. The experimental results are very close to the simulation results. The results show the spectral emittance of plain tungsten is not high enough at short wavelengths such that it cannot be a good TPV emitter.

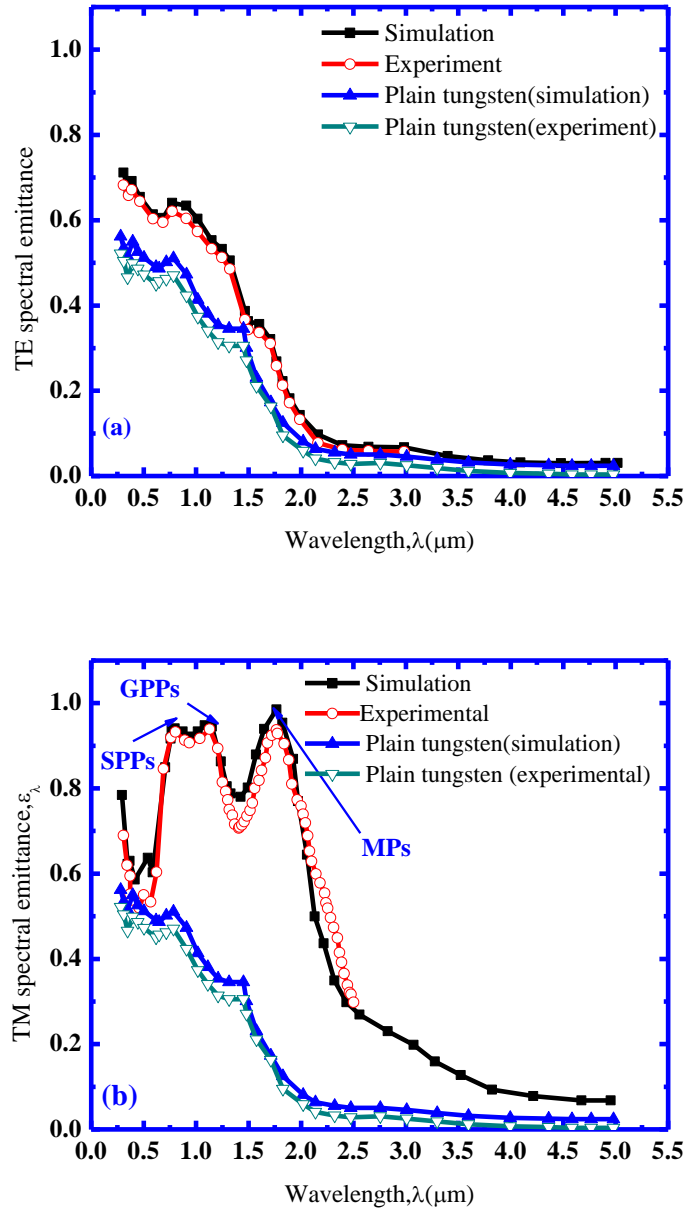


Figure 3. Measured and Simulation spectral emittance of the proposed TPV selective emitter at $\theta = 8^\circ$ for (a) TE (b) TM waves

The bidirectional reflectance distribution function BRDF for the proposed TPV selective emitter at normal incident $\lambda = 660\text{nm}$ was measured by using three-axis automated scatterometer (TAAS) instrument for TE and TM polarization, respectively. The results are plotted in polar coordinates system (where the radial axis denotes zenith angle θ and the polar angle denotes the azimuthal angle ϕ) as shown in Figure 4. The incident laser beam is focused on the sample at spot, which corresponds to the collimator diameter about 5mm and

the blue color in figure denoted to the reflectance places. The results indicated that the proposed TPV selective emitter has the same maximum value of $BRDF \cos\theta$ about 1.2% for both of TE and TM polarization. The measured values of $BRDF \cos\theta$ are very low and the accuracy is not expected be high. When the detector was positioned in front of the laser beam path, it blocks the laser beam and reflectance could not be obtained because of the shadowing effect. It is also noted that the reflected energy at the backward direction is greater than the forward for both of TE and TM polarization.

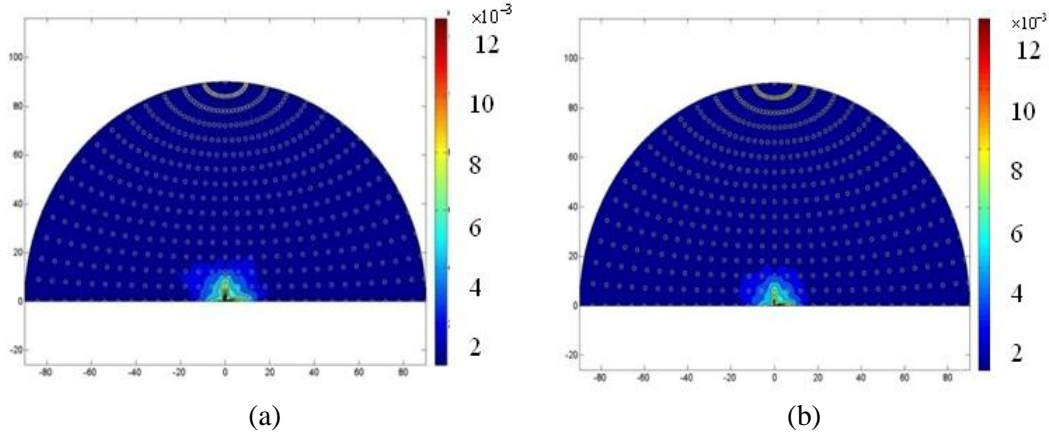


Figure 4. Measured $BRDF \cos\theta$ of the proposed TPV selective emitter at normal incident for (a) TE; (b) TM waves

4.2 Effect of plane of incidence

The effect of the plane of incidence (PoI) on the spectral emittance of the proposed TPV emitter is also studied numerically at different incidence angles for TE and TM waves as shown in Figure 5. The results show that there is hardly any change in the first emittance peak, but the second emittance peak disappears while the third peak moves toward shorter wavelengths, when the angle of incidence is increased from 0 to 60°. It appears that the proposed TPV emitter has high emittance value in near infrared region, so it can be suitable to be used as a wavelength selective emitter in TPV systems.

The effect of the plane of incidence (PoI) on the reflectance distribution $BRDF \cos\theta$ for the proposed TPV selective emitter in the half hemispherical space at different angles (0°, 30° and 60°) was also measured at $\varphi_i = 0^\circ$, $\lambda = 660\text{nm}$ for TM wave as shown in Figure 6. It can be seen from the results that the maximum value of the $BRDF \cos\theta$ at $\theta = 30^\circ$. The maximum value measured of the $BRDF \cos\theta$ at $\theta = 0^\circ$ is very low compared with other incident angles; due to the detector blocking of the laser beam at this angle. The results explained the plane of incidence influence on the $BRDF \cos\theta$ of the proposed TPV emitter. The low reflectance distribution means that it has a high emittance value and this characteristic is desired for the performance of an ideal selective emitter.

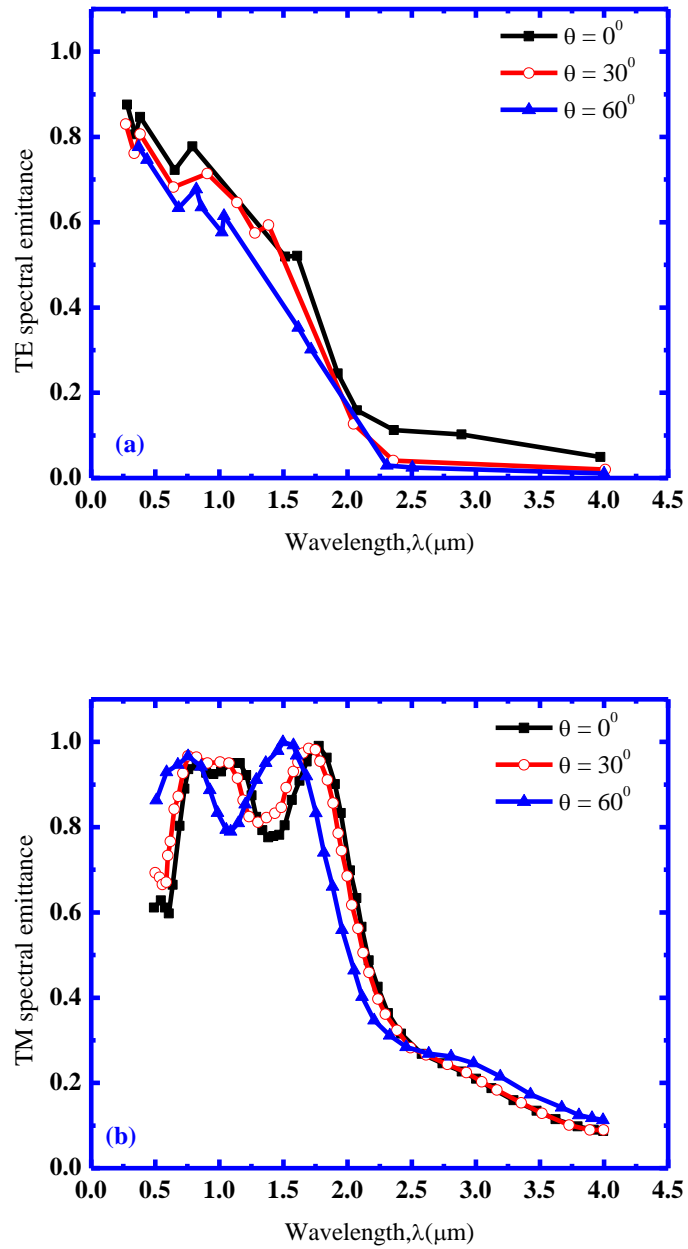


Figure 5. Simulated spectral reflectance at different incident angles for (a) TE; (b) TM waves

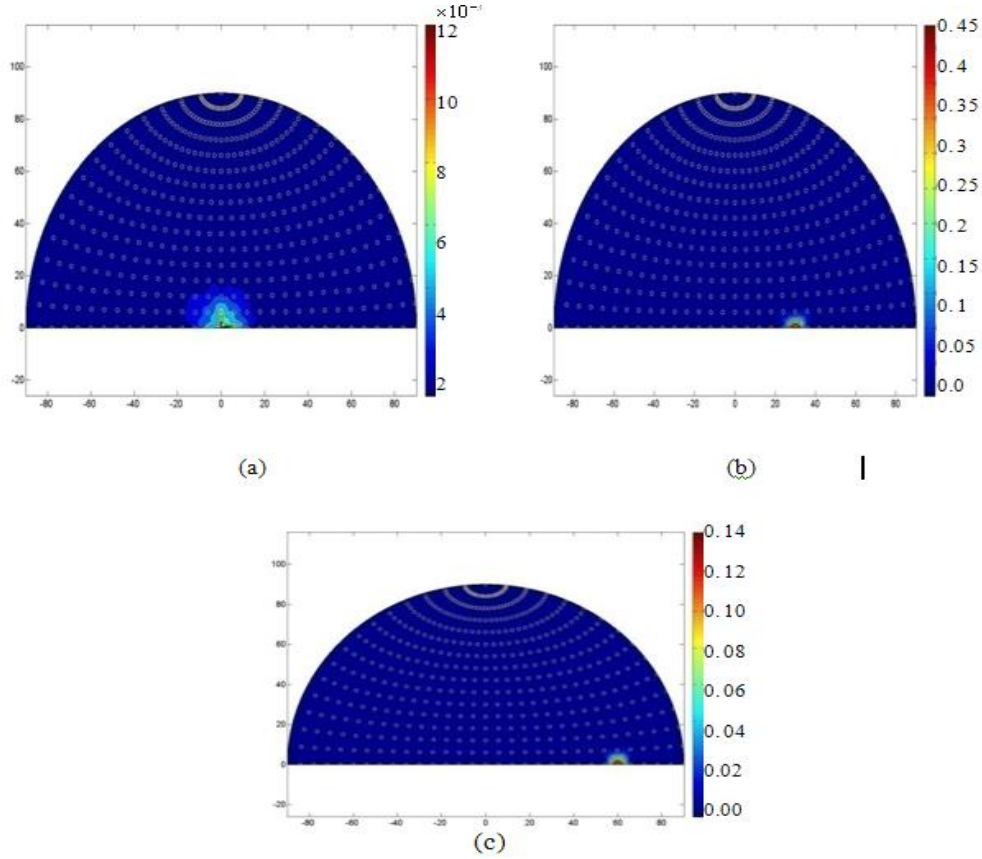


Figure 6. Measured BRDF • cosθ of the proposed TPV selective emitter at different incident angles (a) $\theta = 0^\circ$ (b) $\theta = 30^\circ$ (c) $\theta = 60^\circ$, and $\varphi_i = 0^\circ$ for TM waves

The radiant efficiency of the emitter η_{emt} is defined as the ratio between the net radiation power output from the emitter to the fuel chemical energy input flow can be determined by

$$\eta_{\text{emt}} = \frac{S_E P_{\text{rad}}}{m_{\text{fuel}} \Delta H_L} = \frac{S_E \sigma \varepsilon_{\text{emt}} T_{\text{emt}}^4}{m_{\text{fuel}} \Delta H_L} \quad (10)$$

Where S_E is the surface area of the emitter, P_{rad} is the net radiant power density of the emitter, m_{fuel} the mass flow rate of the fuel and ΔH_L is the low heat value of the fuel.

ΔH_L is taken to be $\text{LHV}_{\text{hydrogen}} = 120.1 \times 10^6 \text{ Jkg}^{-1}$ [10]. If we take as an example the radius (r) and length (L) of the combustor as 1.9mm and 22mm, respectively, the emissive surface area of the cylindrical emitter will be equal to $(S_E = 2\pi rL = 2\pi(1.9\text{mm})(16\text{mm}) = 1.91 \times 10^{-4} \text{ m}^2)$. The radiant efficiency η_{emt} and the emitted power of the emitter as a function of the emitter temperature are shown in Figure 7. The result indicates that the efficiency of the proposed TPV emitter increases as the fourth

power of emitter temperature. The proposed TPV emitter has high radiation power and high efficiency (more than 50%) at emitter temperature higher than 1600 K.

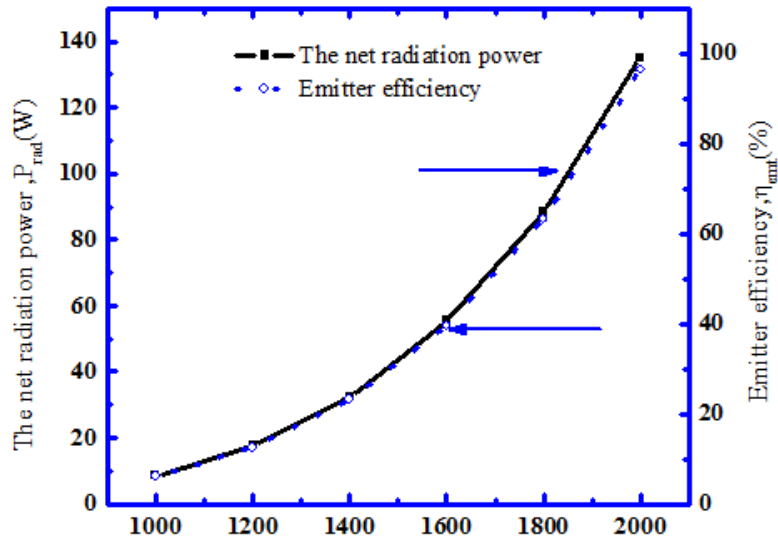


Figure 7. Calculated the net radiation power and efficiency of the proposed TPV emitter at different emitter temperatures

4.3 Spectral properties and BRDF/BTDF measurements for the proposed TPV filter

The spectral reflectance and transmittance of the proposed selective filter was measured at near normal incident 8° and λ from $0.3 \mu\text{m}$ to $2.5 \mu\text{m}$ by using spectral transmittance and reflectance measurement system and also computed numerically at λ from $0.5 \mu\text{m}$ to $5 \mu\text{m}$ as shown in Figure 8. The results show that the selective filter has high reflectance value exceeds 0.4 and 0.7 in both experimentally and simulation, respectively for radiated photons at $\lambda < 1.73 \mu\text{m}$ and high transmittance at this region. It also has highest spectral transmittance experimentally about 0.95 at this region. However it reflects most of the radiated photons at $1.73 \mu\text{m} < \lambda < 3.9 \mu\text{m}$ utilizing the main high reflectance region based on the first stop band which can be shown in the simulation results at wavelength higher than $2.5 \mu\text{m}$. The experimental results are in good agreement with the simulation. Furthermore, there are several peaks and large oscillations appear at $\lambda \leq 1.73 \mu\text{m}$, caused by the refractive index mismatch between the 1D multilayer Si/SiO₂ selective filter and the quartz substrate. These oscillations could lead to poor transmittance in that region. The reducing the first layer of SiO₂ to half of its original thickness to form anti-reflection coating can lead to the increase of pass-band transmittance and improvement the performance of the filter.

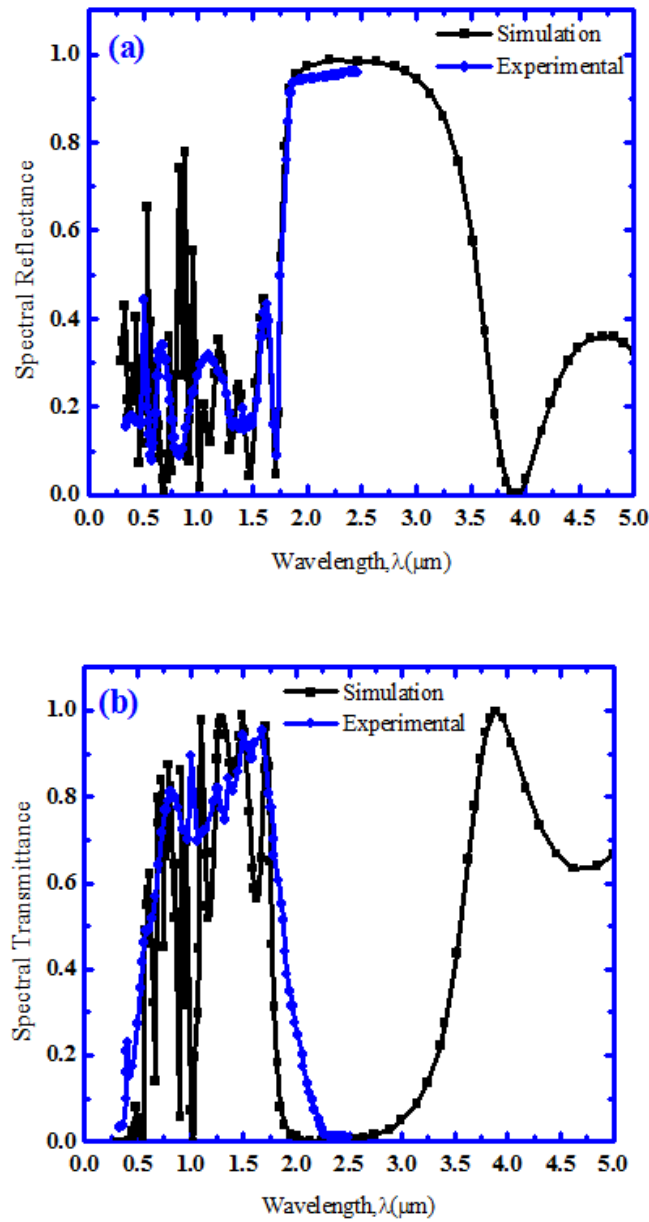


Figure 8. Measured and simulation (a) The spectral reflectance; (b) The spectral transmittance, of the proposed selective filter

The $BRDF \cos \theta$ in the half hemispherical space over the proposed TPV selective filter surface at normal incident $\lambda = 660\text{nm}$ was measured by using TAAS system for TE and TM polarization, respectively, the results are shown in Figure 9. It can be noted that there is no difference in BRDF of this the proposed filter which measured at TE and TM polarization. The results show that the proposed filter has the same maximum value of $BRDF \cos \theta$ about 1.8% for both of TE and TM polarization. It also has low measured $BRDF \cos \theta$ values for TE and TM polarization. The measured $BRDF \cos \theta$ values are inaccurate value

when the laser beam is incident on the proposed filter at $\theta = 0^\circ$ due to detector blocking of the laser beam. Figure 10 shows the measured results of $BTDF \cdot \cos\theta$ of the proposed filter at normal incident for both TE and TM polarization, respectively. As seen from the results, there is no difference in the transmittance distribution of the proposed filter for both of TE and TM polarization. It has the same maximum value of the $BTDF \cdot \cos\theta$ about $80\% < BTDF \cdot \cos\theta < 90\%$ for both of TE and TM polarization. When the laser beam is incident on the proposed filter at $\theta = 0^\circ$ most of the energy is transmitted through it and little part of the energy is reflected and scattered outside of the proposed filter surface.

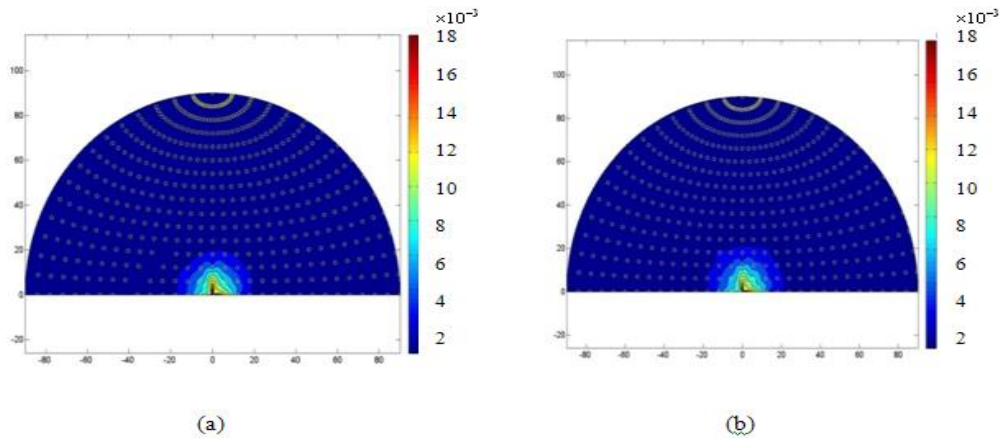


Figure 9. The $BRDF \cdot \cos\theta$ of the proposed TPV selective filter at normal incident for (a) TE; (b) TM waves

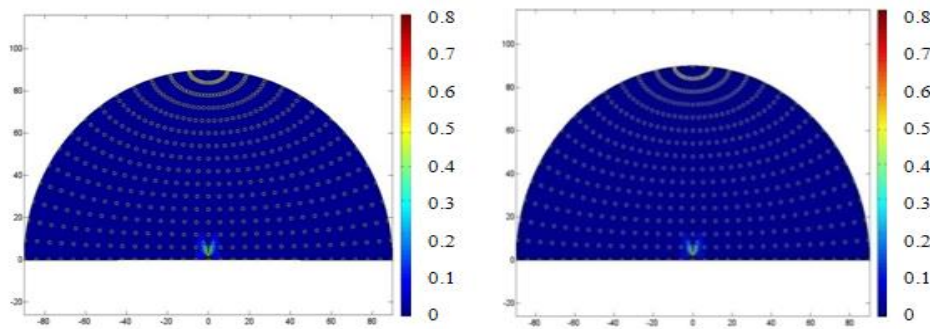


Figure 10. The $BTDF \cdot \cos\theta$ of the proposed TPV selective filter at normal incident for (a) TE; (b) TM waves

5. Conclusion

In order to enhance TPV overall efficiency and output power density we proposed TPV system by using 1D multilayer nanostructure as selective emitter and filter. The spectral radiative properties of these proposed structures are experimentally and theoretically investigated. The spectral emittance of the proposed TPV emitter exhibits three emittance

peaks in our spectral region of interest. These are explained by the mechanisms of the SPPs, GPPs and MPs excitation. The results show that the proposed emitter has high radiation power. The efficiency is more than 50% at emitter temperature greater than 1600 K. The simulated results are in good agreement with the experimental results. The performance of the proposed 1D 4-layer (W/SiO₂) and 1D 8-layer (Si/SiO₂) is suitable to use as selective emitter and filter, respectively with low band gap photovoltaic (GaSb) cell in TPV system applications.

Acknowledgements

This work is supported by the Foundation for Innovative Research Groups of the National Natural Science Foundation of China (No. 51276049) and the Fundamental Research Funds for the Central Universities (No. HIT. BRETIII.201227). A very special acknowledgement is made to the editors and referees whose constructive criticism has improved this paper.

References

- [1] S. Basu, Y.-B. Chen and Z.M. Zhang, *Int. J. of Energy Res.*, vol. 31, (2007).
- [2] L. P. Wang and Z. M. Zhang, *App. Phy. Letts.*, vol. 100, (2012).
- [3] S. I. Mostafa, N. H. Rafat and S.A. El-Naggar, *J. Ren. Energy*, vol. 45, (2012).
- [4] K. Qiu and A. C. S. Hayden, *J. Energy Con. and Management*, vol.47, (2006).
- [5] J. T. Coutts, *J. Ren, Sust. Energy Rev.*, vol. 3, (1999).
- [6] N. Z. Jovanovic, (Thesis), Massachusetts Institute of Technology, (2005).
- [7] W. M. Yang, S. K. Chou, C. Shu, Z. W. Li and H. Xue, *J. Sol, Energy Materials & Sol. Cells*, vol. 80, (2003).
- [8] J. T. Coutts, G. Guazzoni and J. Luther, *Fifth Conference on Thermophotovoltaic Generation of Electricity*, (2002) September 16-19; Rome, Italy.
- [9] D. Kraemer, L. Hu, A. Muto, X. Chen, G. Chen and M. Chiesa, *Appl. Phy. Letts.*, vol. 92, (2008).
- [10] L. C. Chia and B. Feng, *J. Power Sources*, vol. 165, (2007).
- [11] K. Park, S. Basu, W. P. King and Z. M. Zhang, *J. Quan. Spe. & Rad. Trans.*, vol. 109, (2008).
- [12] Y. -B. Chen, (Thesis), Georgia Institute of Technology, (2007) May.
- [13] M. D. Whale, *J. Microscale Thermophysical Engineering*, vol. 5, (2001).
- [14] C. Fu and Z. M. Zhang, *J. Front. Energy Power Eng. China*, vol. 3, (2009).
- [15] J. P. Hesketh, N. J. Zemel and B. Gebhart, *J. Nature*, vol. 324, (1986).
- [16] Y. -B. Chen and Z. M. Zhang, *J. Opt. Commun.*, vol. 269, (2007).
- [17] A. Narayanaswamy and G. Chen, *J. Phys. Rev.*, vol. B70, (2004).
- [18] H. Sai, Y. Kanamori and H. Yugami, *J. Micromechanics and Micro engineering*, vol. 15, (2005).
- [19] P. Nagpal, S. E. Han, A. Stein and D. J. Norris, *Nano Letts.*, vol. 8, (2008).
- [20] X. Liu, T. Tyler, T. Starr, A. F. Starr, N. M. Jokerst and W. J. Padilla, *Phys. Rev. Letts.*, vol. 107, (2011).
- [21] I. Celanovic, F. O'Sullivan, M. Ilak, J. Kassakian and D. Perreault, *Opt. Letts.*, vol. 29, (2004).
- [22] S. Chen, Y. Wang, Y. Duangzheng and Z. Z. Song, *J. Optica Applicata*. XXXIX, (2009).
- [23] M. G. Moharam and T. K. Gaylord, *Opt. Express*, vol. 71, (1981).
- [24] S. Peng and G. M. Morris, *Opt. Express*, vol. 12, (1995).
- [25] V. Badescu, *App. Phy.*, vol. 90, (2001).
- [26] D. Diso, A. Licciulli, A. Bianco, M. Lomascolo, G. Leo, M. Mazzer, S. Tundo, G. Torsello and A. Maffezzoli, *J. Materials Science and Engineering*, vol. B98, (2003).
- [27] H. Sai, H. Yugami, Y. Kanamori and K. Hane, *J. Microscale Thermophys Engineering*, vol. 7, (2003).
- [28] S.Y. Lin, J. Moreno and J. G. Fleming, *App. Phy. Lett.*, vol. 83, (2003).
- [29] E. D. Palik, "Handbook of Optical Constants of Solids", Academic Press, San Diego, CA, (1985).

Authors



Samah G. Babiker

Miss Samah G. Babiker is a PhD student in Harbin Institute of Technology, School of Energy Science and Engineering, Harbin-China. She received an MSc degree in solid state physics from Sudan University of Science and Technology -Khartoum -Sudan in 2009, and BSc degree in Physics Laboratory from the same university in 2006. Her research area of interest is thermo physics, nano/microscale heat transfer.



Mohamed Osman Sid – Ahmed

Prof. Mohamed Osman Sid - Ahmed received Ph. D degree in Solar Energy from University of Reading (UK) in 1981, an MSc degree in Meteorology in 1970, B. Sc degree in Physics in 1967 from the same university Reading- U.K. He worked in department of Meteorology-Khartoum-Sudan from 1970-1975. From 1975-1986 he was Researcher in the Energy Research Institute and National Council for research Khartoum-Sudan. From 1986 -1990, he was an associate Professor and Head of the Applied Physics department- University Gezira-Sudan. From 1990-1994, he was an associate Professor and Head of Wind Energy Department, National Centre for Research, Khartoum-Sudan. From 1994-1996, he was, Dean of Faculty of Education, University of El-Fashir-Sudan. From 1997-2003 he was, Head of physics Department, Hail T. College, Saudi Arabia. From 2003-2005 he was, Head of physics Department- Sudan Univ. of Science and Technology .He is currently a professor of physics, Physics Dept., Sudan Univ. of Science and Technology, Khartoum-Sudan. His research interests are radiative heat transfer and organic solar cells, Renewable Energy.



Shuai Yong

Dr. Shuai Yong is an associate professor at Harbin Institute of Technology. He got his PhD degree from Harbin Institute of Technology in 2009. He worked as a visiting scholar in 2011-2012 at Georgia Institute of Technology. His research is centered on nano/microscale heat transfer, and solar thermal utilization.



Xie Ming

Prof. Xie Ming received the Ph.D. degree in School of Energy Science and Technology from Harbin Institute of Technology (HIT) in Harbin, China in 2006. From 1984 to 1986, he worked at HIT as an associate engineer. From 1986 to 1994, he was a lecturer at the Department of Civil Engineering of HIT. From 1995 to 2001, he was an associate professor at the Department of Civil Engineering, HIT, and served as the vice president of this department during 1997 to 2000. He is currently a professor of engineering thermal physics at School of Energy Science and Technology, Harbin Institute of Technology, China. His research interests are radiative heat transfer and coupled heat transfer, surface radiation and particle radiation characteristics, target infrared model, and air conditioning systems.